

Sharp fronts in attracting-atom monolayers

G.G. Izús^{1,a} and R.R. Deza^{1,b}, and H.S. Wio^{2,c}

¹ IFIMAR (UNMDP-CONICET), Funes 3350, 7600 Mar del Plata, Argentina

² IFCA (UC-CSIC), Avda. de los Castros s/n, E-39005 Santander, Spain

Received 11 September 2013 / Received in final form 25 November 2013

Published online xx January 2014

Abstract. The problem of pattern formation by adsorbates undergoing attractive lateral interactions, is described by a parabolic integrodifferential equation having the scaled inverse temperature ϵ and the scaled pressure α of the vapor phase as parameters. A coexistence region of high- and low-coverage stable homogeneous states has been reported in the (ϵ, α) plane. In the small interaction-range limit an *effective* diffusion coefficient can be defined, which becomes however *negative* for a coverage range in between the stable homogeneous ones.

A novel free-energy-like Lyapunov functional is found here for this problem. When evaluated on the homogeneous states, it leads to a Maxwell-like construction which selects essentially the same value $\alpha(\epsilon)$ as the originally posited zero front-velocity condition. Moreover, its value on static fronts at this particular $\alpha(\epsilon)$ coincides with those of the homogeneous states. This article is dedicated to Prof. Helmut Brand with occasion of his 60th birthday.

1 Introduction

Reaction–diffusion (RD) modeling of patterns on adsorbed monolayers was rightful up to the mid nineties [1,2], since with the resolution achieved by *photoelectron emission microscopy* (PEEM), only structures with characteristic length scales larger than the reactants' diffusion lengths could be seen. The development of novel experimental techniques allowing atomic resolution in real time, such as *field ion microscopy* and fast *scanning tunneling microscopy* (STM) [3–5], has revealed fast kinetic processes that typically lead to nanoscale patterns (such as spots and *micro-reactors* [6–8]) which cannot anymore be described by RD models.

It was by the mid nineties that Mikhailov, Ertl and collaborators realized that the abovementioned fast kinetic processes on the adsorbed monolayers were driven by attractive lateral interactions between adatoms, and wrote up a mesoscopic, field-theoretic model (although not a RD one) for the coverage $c(\mathbf{r}, t)$, first on phenomenological grounds [9,10] and then backed up by a microscopic description [6]. The first application of this new theory—generalized afterward to more layers [11]—was

^a e-mail: izus@mdp.edu.ar

^b e-mail: deza@mdp.edu.ar

^c e-mail: wio@ifca.unican.es

stationary traveling fronts. In the small interaction-range limit and outside the front's core, these patterns admit an *effective* RD description which (as argued in Ref. [10] and shown below) is however not describable by means of a Ginzburg–Landau functional (model A according to [12])¹ and whose “reaction” term describes the struggle between adsorption and desorption chemical potentials (an equilibrium process whose fluctuations would be of additive thermal character). On the other hand, it is easy to see that fluctuations in parameter α (the scaled pressure of the vapor phase) lead to a multiplicative process calling for a more sophisticated framework, namely a *non-equilibrium potential* (NEP).

A restricted NEP (applicable only to *homogeneous* states in this limit) was found in Ref. [13] and applied to stochastic resonance (SR) between high- and low-coverage situations, under adiabatic harmonic variation of the vapor pressure. As a first step towards the analysis of truly *localized* patterns as spots and microreactors, it was our aim in this work to further that finding and seek a full NEP able to describe SR between moving fronts under adiabatic “rocking” of α . Whereas that goal proved to be too ambitious, we have found a novel free-energy-like Lyapunov functional which yields meaningful results when applied to fronts and sheds some light on theoretical aspects. Although its practical applicability is somewhat reduced (it would apply e.g. to a case in which the coverage itself is perturbed, a situation which is not experimentally practicable as it is to perturb the vapor phase pressure), it does allow to characterize noise-assisted phenomena from a NEP framework.

In Sect. 2 we introduce the model and its small interaction-range limit. Section 3 is devoted to the homogeneous states: we revisit the NEP found in Ref. [13] and state an alternative free-energy-like Lyapunov functional which we evaluate on them. Section 4 is in turn devoted to fronts: we regard them under the light of this new functional, and compare the obtained results with the $V = 0$ criterion of Ref. [9]. Conclusions are outlined in Sect. 5, together with an outlook of work in course.

2 Single monolayer with adatom attraction

2.1 The general setup

In Ref. [9] it was recognized that the time scale of the problem is set by the adatom's residence time t_d in the monolayer, namely the inverse of the desorption rate k_d . Because of adatom attraction—described by a field $U(\mathbf{r}, t)$ which is a functional of $c(\mathbf{r}, t)$ —the single-adatom rate $k_{d,0}$ is strongly depressed by a factor $\exp(U/k_B T)$. So we shall work with a scaled time variable $\tau = t/t_d$, t being the physical time variable.

Regarding space scales, *two* of them are relevant:

- One is of course the *diffusion length* $L_{\text{diff}} = D/k_{d,0}$ (with D the diffusion coefficient), by which the physical time variable will be scaled: $\xi = |\mathbf{r}|/L_{\text{diff}}$.
- The other one is the *range* of the inter-adatom attractive potential $u(\mathbf{r})$. This is relevant for the calculation of the field entering the depressing factor of $k_{d,0}$, which in the mean-field approximation reads

$$U(\mathbf{r}, t) = - \int d\mathbf{r}' u(\mathbf{r} - \mathbf{r}') c(\mathbf{r}', t).$$

We shall work in the scaled space (ξ) and time (τ) variables, which leads in turn to define scaled coefficients $\alpha = k_a p/k_{d,0}$ (with k_a the adsorption rate and p the physical

¹ A Cahn–Hilliard (model B) description does not apply, since whereas the on-surface process conserves the order parameter c , the adsorption–desorption one does not.

vapor pressure) and $\epsilon = u_0/k_B T$, with $u_0 = \int d\mathbf{r} u(\mathbf{r})$ the attractive interaction strength. Following [9,10], in this work we restrict ourselves to *flat* fronts, and so we omit the transversal dimension whilst assuming an infinite ξ domain in order to avoid contributions to the NEP from the boundary conditions. Moreover, assuming as in Ref. [9] the ubiquitous Gaussian form for $u(\mathbf{r})$ with variance $l_0^2/2$, namely $u(r) = u_0 f(r)$ with $f(r) = (\pi l_0^2)^{-1} \exp(-r^2/l_0^2)$, the evolution equation for the coverage $c(\xi, \tau)$ reads [9]

$$\begin{aligned} \partial_\tau c = & \alpha(1-c) - c \exp \left[-\epsilon \int_{-\infty}^{\infty} d\xi' f(\xi - \xi') c(\xi', t) \right] \\ & + \partial_\xi \left[-\epsilon c(1-c) \partial_\xi \int_{-\infty}^{\infty} d\xi' f(\xi - \xi') c(\xi', t) + \partial_\xi c \right]. \end{aligned} \quad (1)$$

The factor $(1-c)$ accounts for the obvious fact that microscopically, adatoms in monolayers can only occupy void sites. The terms in the first line account for adsorption and desorption, the second term in the second line for normal diffusion, and the first one for new ingredient of the theory—the aggregating current (induced by adatom attraction) which counteracts it.

2.2 The small interaction-range limit

The small interaction-range limit of Eq. (1) was found in Ref. [9] by assuming for $u(\mathbf{r})$ the ubiquitous Gaussian form, with variance $l_0^2/2$. This expression is known to tend to $\delta(\mathbf{r})$ as $l_0 \rightarrow 0$. An alternative derivation, making for $u(\mathbf{r})$ no assumption other than analyticity, has been worked out in Ref. [13]. In that limit, Eq. (1) reduces to

$$\partial_\tau c = \alpha(1-c) - c e^{-\epsilon c} - \partial_\xi [\epsilon c(1-c) \partial_\xi c] + \partial_{\xi\xi} c. \quad (2)$$

This can be *formally* written as a (field-dependent) diffusion–reaction equation

$$\partial_\tau c = g(c) + \partial_\xi [D_{\text{eff}}(c) \partial_\xi c], \quad (3)$$

with

$$g(c) := \alpha(1-c) - c e^{-\epsilon c} \quad , \quad D_{\text{eff}}(c) := 1 - \epsilon c(1-c), \quad (4)$$

if we allow $D_{\text{eff}}(c)$ to become negative. This occurs for $\epsilon > 4$ in a coverage range lying between

$$c_\pm(\epsilon) = \frac{1}{2} \left(1 \pm \sqrt{1 - 4/\epsilon} \right). \quad (5)$$

Hereafter we shall deal only with *stationary* solutions of Eq. (3), a class which includes not only *static* ($\partial_\tau c = 0$) ones but also those depending only on $\zeta = \xi - V\tau$ ($V = \text{const}$), for which Eq. (3) reads

$$\partial_\zeta [D_{\text{eff}}(c) \partial_\zeta c + Vc] + g(c) = 0. \quad (6)$$

3 Homogeneous states and nonequilibrium potentials

3.1 Homogeneous states

- For $\epsilon > 4$ and $\alpha_{\min}(\epsilon) < \alpha < \alpha_{\max}(\epsilon)$, $g(c)$ exhibits *two* stable roots $c_1(\epsilon, \alpha)$ and $c_3(\epsilon, \alpha)$, which lie outside $[c_-(\epsilon), c_+(\epsilon)]$.

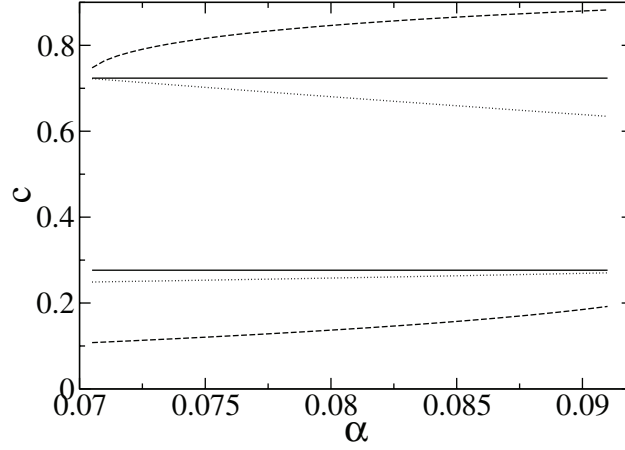


Fig. 1. Stable homogeneous coverages c_1 and c_3 (dashed lines), locus of binodals \tilde{c}_1 and \tilde{c}_3 (dotted lines) and boundaries of $D_{\text{eff}}(c) < 0$ region (solid lines) as functions of α , for $\epsilon = 5.0$.

- At $\alpha_{\min}(\epsilon)$ it is $c_1(\epsilon, \alpha) = c_-(\epsilon)$ and at $\alpha_{\max}(\epsilon)$, $c_3(\epsilon, \alpha) = c_+(\epsilon)$.
- For $\alpha < \alpha_{\min}(\epsilon)$ [$\alpha > \alpha_{\max}(\epsilon)$] only $c_1(\epsilon, \alpha)$ [$c_3(\epsilon, \alpha)$] survives and the process is effectively a diffusion–reaction one (in the small interaction-range limit, recall).

In order to clarify the relation (if any) between the $V = 0$ condition in Ref. [9] and a Maxwell construction, it is useful to represent (in addition to c_1 , c_3 , c_- and c_+) the position of the binodals \tilde{c}_1 and \tilde{c}_3 [the roots of $g'(c)$, with $' \equiv d/dc$] as functions of $\alpha \in [\alpha_{\min}, \alpha_{\max}]$ for fixed ϵ . That is done for $\epsilon = 5$ in Fig. 1, where \tilde{c}_1 and \tilde{c}_3 (dotted lines) are seen to keep no relation with c_- and c_+ (solid lines) however near them they lie. The positions of c_1 and c_3 are indicated with dashed lines.

3.2 A restricted NEP for homogeneous states

The true dimension of the NEP concept $\Phi(\mathbf{q})$, defined through [14]

$$\lim_{\nu \rightarrow 0} P_{\text{stat}}(\mathbf{q}; \nu) = Z(\mathbf{q}) \exp \left[-\frac{\Phi(\mathbf{q})}{\nu} \right],$$

becomes fully appreciated only for *multiplicative* noise. We note first that whereas c has the meaning of an order parameter, the true (experimentally accessible) thermodynamic variables are ϵ and α . If α is assumed to undergo Gaussian fluctuations around a fixed value,

$$\alpha = \alpha_0 + \sqrt{\nu} \eta(\tau), \quad \text{with } \langle \eta(\tau) \rangle = 0 \text{ and } \langle \eta(\tau) \eta(\tau') \rangle = 2\delta(\tau - \tau'),$$

one ends up with the Langevin-like stochastic differential equation (SDE)

$$\dot{c} = g(c) + \sqrt{\nu} (1 - c) \eta(\tau)$$

(the dot stands obviously for $d/d\tau$). The equation defining the NEP $\Phi(c)$ is thus [14]

$$g(c) \Phi'(c) + [(1 - c) \Phi'(c)]^2 = 0,$$

with the nontrivial solution

$$\Phi(c) = \alpha_0 \ln(1 - c) + \int_0^c \frac{z e^{-\epsilon z} dz}{(1 - z)^2}. \quad (7)$$

The second term yields

$$\left[\frac{e^{-\epsilon c}}{(1-c)} - 1 \right] + (1-\epsilon) e^{-\epsilon} \{ \text{Ei}[\epsilon(1-c)] - \text{Ei}(\epsilon) \}, \quad (8)$$

with $\text{Ei}(x) = -\int_{-x}^{\infty} e^{-z} z^{-1} dz$, which agrees with Eq. (12) in Ref. [13] (where the lower integration limits build up the normalization factor \mathcal{N}). Regarding the first one, one might lump it into $Z(\mathbf{q})$ without further ado. However, it is important to realize that since the diffusion term in the SDE tends to $\sqrt{\nu} \eta(\tau)$ for $c \rightarrow 0$, one must recover the additive-noise NEP (see below) through a Taylor expansion of Eq. (7),

$$\Phi(c) \approx -\int_0^c [\alpha_0(1-z) - z e^{-\epsilon z}] dz = -\int_0^c g(z) dz := \mu(c),$$

namely the process' chemical potential (denoted as $U_{\text{eff}}(c)$ in Ref. [13]). A quantitative evaluation shows however that already for $c \approx c_1(\epsilon = 5, \alpha = 0.088)$, the deviation between both expressions is important.

3.3 In search of a NEP applicable to fronts

As a first step, we switch to the simpler task of finding such a NEP under additive noise. We thus seek a functional $\mathcal{F}[c]$ from which the (pseudo) reaction–diffusion problem with field-dependent diffusion coefficient

$$\partial_\tau c = g(c) + \partial_\xi [D_{\text{eff}}(c) \partial_\xi c] = g(c) + D_{\text{eff}}(c) \partial_{\xi\xi} c + D'_{\text{eff}}(c) (\partial_\xi c)^2 \quad (9)$$

could be variationally derived. As argued in Ref. [10], the usual approach

$$\partial_\tau c = -\frac{1}{D_{\text{eff}}(c)} \frac{\delta \mathcal{F}_1[c]}{\delta c(\xi)} \quad (10)$$

with

$$\mathcal{F}_1[c] := \int_{-\infty}^{\infty} \left\{ \frac{1}{2} [D_{\text{eff}}(c) \partial_\xi c]^2 - G(c) \right\} d\xi \quad (11)$$

playing the role of a Ginzburg–Landau functional for field-dependent diffusion and

$$G(c) := \int_0^c D_{\text{eff}}(z) g(z) dz$$

does not work here, in the sense that $\mathcal{F}_1[c]$ will not be a Lyapunov functional where $D_{\text{eff}}(c) < 0$ [in other words, $\dot{\mathcal{F}}_1[c] \leq 0$ is not guaranteed for $c_-(\epsilon) < c < c_+(\epsilon)$]. Since the NEP is meant to describe fluctuations, there is no way the interval $[c_-(\epsilon), c_+(\epsilon)]$ could be avoided.

We try out finding a functional $\mathcal{F}_2[c]$ such that

$$\partial_\tau c = -\frac{\delta \mathcal{F}_2[c]}{\delta c(\xi)}. \quad (12)$$

Clearly, the “reaction” term in $\mathcal{F}_2[c]$ will be $\mu(c)$. For the “kinetic” term we propose

$$\mathcal{K}_2^{(\xi)}[c] := -\int_{-\infty}^{\infty} c \partial_\xi [D_{\text{eff}}(c) \partial_\xi c] d\xi, \quad (13)$$

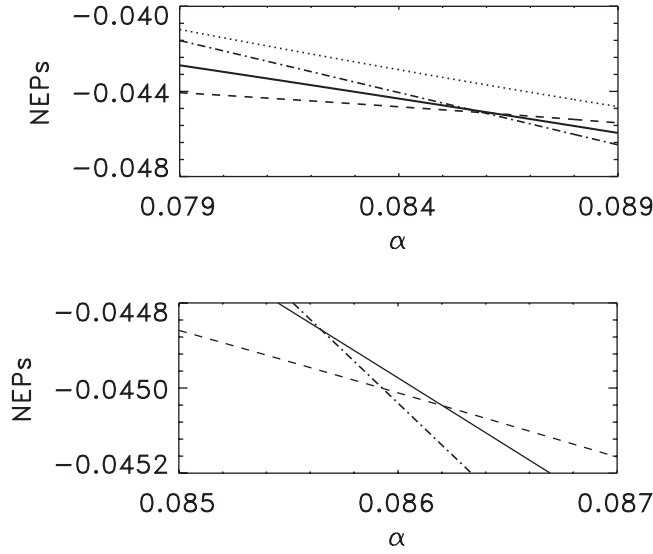


Fig. 2. The NEP from Eq. (14) evaluated at c_1 (dashed line), c_3 (dot-dashed line), c_2 (dotted line) and the front (solid line) as functions of α , for $\epsilon = 5.0$.

whose variation with respect to c yields

$$\delta\mathcal{K}_2^{(\xi)}[c] = - \int_{-\infty}^{\infty} \{[\partial_{\xi}(D_{\text{eff}}\partial_{\xi}c)]\delta c + c\delta[\partial_{\xi}(D_{\text{eff}}\partial_{\xi}c)]\}d\xi.$$

Now, the second term can be shown to vanish. Hence

$$\mathcal{F}_2[c] := \int_{-\infty}^{\infty} \{c\partial_{\xi}[D_{\text{eff}}(c)\partial_{\xi}c] + \mu(c)\}d\xi \quad (14)$$

fulfills Eq. (12) and is moreover a Lyapunov functional,

$$\dot{\mathcal{F}}_2 = \int_{-\infty}^{\infty} \left(\frac{\delta\mathcal{F}}{\delta c}\right)(\partial_{\tau}c)d\xi = - \int_{-\infty}^{\infty} \left(\frac{\delta\mathcal{F}}{\delta c}\right)^2 d\xi \leq 0, \quad (15)$$

even for *non-positive* diffusion coefficient. In Fig. 2, $\mathcal{F}_2[c]$ is evaluated on the homogeneous states: the stable ones c_1 (dashed line) and c_3 (dot-dashed line), and the unstable one c_2 (dotted line), for α values in the coexistence region for $\epsilon = 5$. A stability exchange is observed at $\alpha \approx 0.086$.

4 Fronts

Front solutions to Eq. (6) were analyzed in Ref. [9], whose authors arrived at

$$V = \frac{[G(c_3) - G(c_1)] - [G(c_+) - G(c_-)]}{\mathcal{K}^{(\zeta)}[c]}. \quad (16)$$

The denominator

$$\mathcal{K}^{(\zeta)}[c] = \int_{-\infty}^{\infty} D_{\text{eff}}(\partial_{\zeta}c)^2 d\zeta,$$

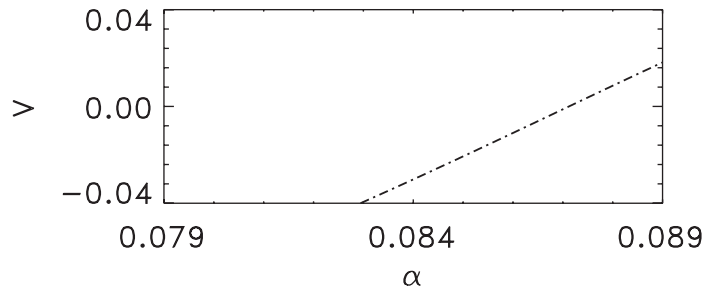


Fig. 3. Front velocity from Eq. (16) as a function of α , for $\epsilon = 5.0$.

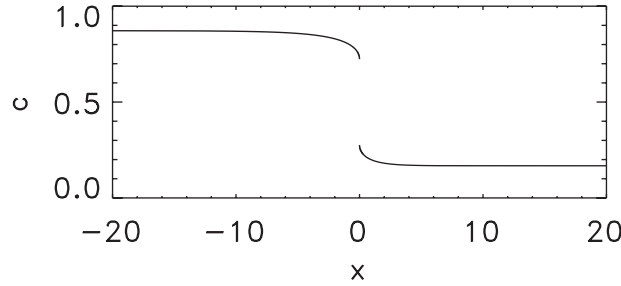


Fig. 4. Static coverage profile in the monolayer case, for $\epsilon = 5.0$ and $\alpha \approx 0.088$.

evaluated on the profile $c(\zeta)$ moving at constant speed V , must in general be evaluated numerically². That has been done in Fig. 3, where V calculated from Eq. (16) is plotted *vs* α in the coexistence region, for $\epsilon = 5$. As seen, $V = 0$ occurs at $\alpha \approx 0.088$, not very far from the stability-exchange point of homogeneous states, according to $\mathcal{F}_2[c]$.

For $V = 0$, Eq. (6) tells us that it admits a solution by quadrature (we may think of $\mathcal{F}_1[c]$ as an “action” and $\frac{1}{2}[D_{\text{eff}}(c) \partial_\xi c]^2 + G(c)$ as an “energy”)

$$\xi(c) = \int_c^{c_-} \frac{D_{\text{eff}}(z) dz}{\sqrt{2[G(c_1) - G(z)]}} \quad \text{for } c_1 < c < c_-, \quad (17)$$

$$\xi(c) = - \int_{c_+}^c \frac{D_{\text{eff}}(z) dz}{\sqrt{2[G(c_3) - G(z)]}} \quad \text{for } c_+ < c < c_3, \quad (18)$$

whose profile is depicted in Fig. 4. Now, the curve of $\mathcal{F}_2[c]$ evaluated at this solution (solid line in the upper frame of Fig. 2) passes near the stability-exchange point of homogeneous states, as shown in the lower frame of Fig. 2.

Following the steps that led to Eq. (16), but multiplying Eq. (6) this time only by $\partial_\zeta c$, we get

$$V = \frac{[\mu(c_3) - \mu(c_1)] - [\mu(c_+) - \mu(c_-)] - \frac{1}{2} \int_{-\infty}^{\infty} D'_{\text{eff}} (\partial_\zeta c)^3 d\zeta}{\int_{-\infty}^{\infty} (\partial_\zeta c)^2 d\zeta}, \quad (19)$$

which has the further advantage of isolating the front core contribution from those of the c_1 and c_3 domains.

² $\mathcal{K}_2^{(\zeta)}[c]$ —the one from Eq. (13), evaluated on $c(\zeta)$ moving at speed V —and $\mathcal{K}^{(\zeta)}[c]$ can be shown to be numerically equivalent after integration by parts. Note that $D_{\text{eff}} < 0$ does not occur in $\mathcal{K}^{(\zeta)}[c]$, because of the abrupt jump from $c_+(\epsilon)$ to $c_-(\epsilon)$.

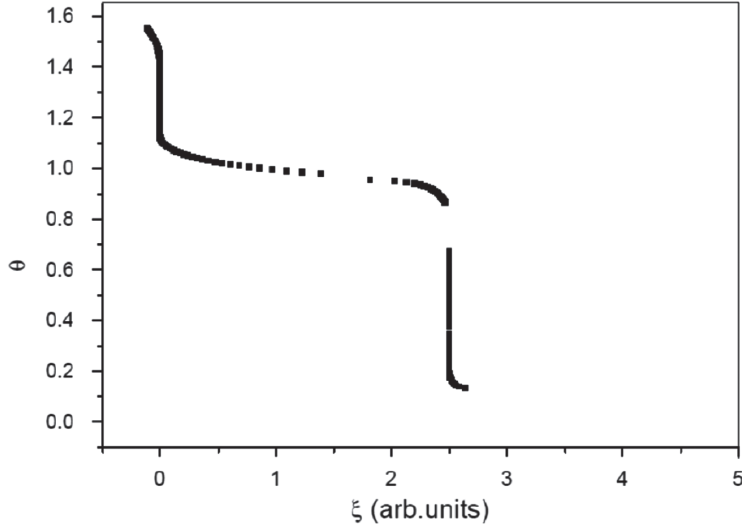


Fig. 5. A typical static coverage profile arising in the multilayer case (adapted from Ref. [11] and indicated by θ). Parameters: $\epsilon = 5.6$, $\alpha_1 = 0.08$ and $\alpha_2 = 0.096$.

5 Conclusions and outlook

In order to study noise-induced effects, we have obtained a novel free-energy-like Lyapunov functional, a *nonequilibrium potential*, for an adsorption–desorption system. It yields meaningful results when applied to fronts and also helps shed light on theoretical aspects. Although its practical applicability is somewhat restricted, it does allow characterizing noise-assisted phenomena within a NEP framework, whose 2D generalization is straightforward, although curvature effects are expected. It considers the adsorption–desorption process as a spatiotemporal white noise (as in KPZ) which can create opposite-phase domains and also change the front location.

Here we have focused on the adsorbate monolayer case. In [11], a generalization to the multilayer situation has been undertaken. We are presently looking at the double-layer system, which in unnormalized variables reads

$$\begin{aligned} \partial_t c_1(x, t) &= \{k_a p (1 - c_1) - k_{d,0} c_1 \exp[U_1(x)/T] + k_T c_1\} (1 - c_2) \\ &\quad + \partial_x \left(\frac{D}{T} U'_1(x) c_1 (1 - c_1) + D \partial_x c_1 \right), \\ \partial_t c_2(x, t) &= k'_a p c_1 (1 - c_2) - k'_{d,0} c_2 \exp[U_2(x)/T] + k'_T c_2 (1 - c_1) \\ &\quad + \partial_x \left(\frac{D}{T} U'_2(x) c_2 (1 - c_2) + D \partial_x c_2 \right), \end{aligned} \quad (20)$$

from the NEP perspective. Subscript 1 indicates the innermost layer (the one directly attached to the metallic surface) and 2 the outer one. Adsorption and bare desorption rates for the outer layer are indicated with a prime. A new mechanism working here is *transfer* between layers, involving *free* sites in the target layer and *occupied* sites in the initial one and characterized by the coupling parameters k_T for outward transfer [$k_T c_1 (1 - c_2)$] and k'_T for inward transfer [$k'_T c_2 (1 - c_1)$]. Typically, stepped profiles result within this model [11], as the one shown in Fig. 5.

If a NEP is obtained for this generalization (even with restricted validity as in the present case) it will open the possibility of analyzing noise effects in *wetting*-related problems. Our advances on the subject will be reported elsewhere.

We thank the editors for inviting us to participate in this volume. Financial support from UNMDP and CONICET (PIP No 12220100315) of Argentina, and from MINECO (FIS2010-18023) of Spain, is acknowledged.

References

1. M.C. Cross, P.C. Hohenberg, *Rev. Mod. Phys.* **65**, 851 (1993)
2. R. Kapral, K. Showalter (ed.), *Chemical Waves and Patterns* (Kluwer, Dordrecht, 1993)
3. J. Trost, T. Zambelli, J. Winterlin, G. Ertl, *Phys. Rev. B* **54**, 17850 (1996)
4. J. Winterlin, S. Völkening, T.V.W. Janssens, T. Zambelli, G. Ertl, *Science* **278**, 1931 (1997)
5. S. Völkening, K. Bedürftig, K. Jacobi, J. Winterlin, G. Ertl, *Phys. Rev. Lett.* **83**, 2672 (1999)
6. M. Hildebrand, A.S. Mikhailov, *J. Phys. Chem.* **100**, 19089 (1996)
7. D. Battogtokh, M. Hildebrand, K. Krischer, A.S. Mikhailov, *Phys. Rep.* **288**, 435 (1997)
8. M. Hildebrand, M. Kuperman, H.S. Wio, A.S. Mikhailov, G. Ertl, *Phys. Rev. Lett.* **83**, 1475 (1999)
9. A. Mikhailov, G. Ertl, *Chem. Phys. Lett.* **238**, 104 (1995)
10. A. Mikhailov, G. Ertl, *Chem. Phys. Lett.* **267**, 400 (1997)
11. S.B. Casal, H.S. Wio, S.E. Mangioni, *Physica A* **311**, 443 (2002)
12. P. Hohenberg, B. Halperin, *Rev. Mod. Phys.* **49**, 435 (1977)
13. J.A. Sierra, H.S. Wio, *Central Eur. J. Phys.* **10**, 625 (2012)
14. H.S. Wio, R.R. Deza, *Eur. Phys. J. Special Topics* **146**, 111 (2007)

